Design of an electromagnetic-transducer energy harvester

L Simeone*, M Ghandchi Tehrani and S J Elliott

Institute of Sound and Vibration Research, University of Southampton, SO17 1BJ, United Kingdom

*Author to whom any correspondence should be addressed

ls2n12@soton.ac.uk

Abstract. This paper presents the design and the manufacturing of an electromagnetic-transducer energy harvester. The design considers the coupling between the mechanical vibrating behaviour, generated by a base excitation, and the electromagnetic conversion of energy, which is aimed to produce the voltage across a load resistance. The design is based on some constraints, which are related to the characteristics of the shaker and aimed to obtain the best performance of the device. Current tests show the presence friction at low input levels, which is associated with the gearbox. The output voltage and the harvested power of the device are studied experimentally for different values of load. By increasing the value of the load from zero (short circuit) to high values (open circuit) the swing angle increases, while the harvested power presents a peak associated with the electrical damping. Also, harmonic tests are run at resonance for different levels of excitation to demonstrate the effect of the nonlinearity on the voltage and the harvested power. A nonlinear load resistance, is then introduced as part of future work. The aim is to try to increase the harvested power with respect to the linear load, at low level of excitation.

1. Introduction

In several applications such as the motion of the sea waves [1] and the rotation of the rotor in helicopters [2], the source of excitation is characterised by a narrow frequency bandwidth and, as a consequence, the excitation can be approximated as harmonic. Moreover, a harmonic analysis is always the starting point to design a new mechanical system [1, 3-9]. In order to increase the performance, over which the vibration energy harvester operates, various nonlinear arrangements were suggested, particularly using nonlinear springs [4, 10]. In contrast, it was recently shown that the dynamic range of a vibration energy harvester can be increased using a nonlinear damper. For example, Ghandchi Tehrani and Elliott [5] introduced the use of the cubic damping for enlarging the dynamic range of performance of an energy-harvesting device. It was shown that a shunted cubic resistance generates cubic damping into the system, which is a fourth power function of the torque constant. The authors demonstrated that the harvested power obtained by using a cubic damper can be significantly larger than that of a linear harvesting device when excited at resonance, at amplitudes below its maximum operational limit Y_{max}. An important study was conducted in [11]. The authors studied an energy harvester with an internal resistance in series with a cubic load. It was found that the internal resistance provides an upper limit for the electrical damping when using a nonlinear load. In addition, at high levels of excitation, the harvester behaves linearly, while, the behaviour becomes

more similar to a harvester with purely nonlinear damping as long as the input level decreases. However, no experimental results were reported in this study.
This paper presents the design of a constrained electromagnetic transducer energy harvester. The work is aimed to show that the use of a gearbox to increase the output voltage also increases the amount of mechanical damping into the system. Also, the effect of a linear load on the output voltage and the harvested power is estimated experimentally. The last section is dedicated to the introduction of a nonlinear load, which is aimed to increase the harvested power over the dynamic range of the harvester.

2. Design of rotational energy harvester

The harvester is designed to behave like a single-degree-of-freedom pendulum, as shown in Figure 2. The system can rotate by means of a hinge on the left side, while on the right side, a lumped mass M is attached to the beam of mass m. The moment of inertia associated with the rotation of the masses is indicated with J. The system is connected to the ground by a spring k and is subjected to a base excitation y through a shaker. The hinge is connected to a gear box and a generator, which couples the mechanical and the electrical circuit. DC motor and gear box also provide a large amount of mechanical damping, that can be split in both viscous c_m and friction τ_s. The rotational motion is used to produce voltage across a load and, therefore, harvested power. The device is designed to be harmonically excited, even though other types of excitation will also be considered in the future. Assuming that an electrical generator with emf-constant K_t and an internal reistance R_i is coupled to the mechanical system, then a current i is induced in the electrical circuit, when a swing rotation θ is produced by the base motion. The harvesting process can start when a load R_l is attached to the terminals of the motor.

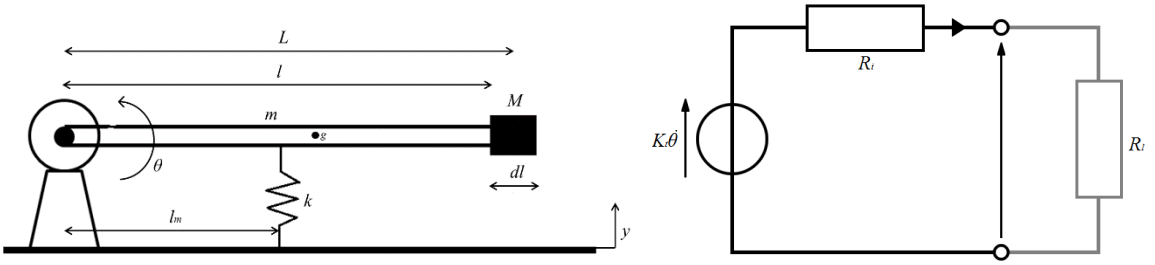

Figure 1: Electromagnetic energy harvester

The general behaviour of the coupled system can be described as

$$J\ddot{\theta} + c_m\dot{\theta} + \tau_s sign(\dot{\theta}) + kl_m^2\theta + K_t i = -\left(ml/2 + M\left(l + dl/2\right)\right)\ddot{y}, \tag{1}$$

$$K_t\dot{\theta} = \left(R_i + R_l\right)i \tag{2}$$

Where l_m is the position of the spring with respect to the hinge, l is the length of the beam and dl is the length of the cuboid lumped mass. The first equation is referred to the mechanical circuit, while the second equation, describes the dynamics of the electrical circuit, in which only the effect of the internal resistance and the load resistance was considered, and the capacity, as well as the inductance, were neglected since they do not affect the system at the frequency of interest.
For harmonic base excitation $y = Y\sin(\omega t - \varphi)$, the amplitude of the angular displacement Θ can be obtained by using the harmonic balance method as

$$\left|\frac{\Theta}{Y}\right| = \frac{\left(ml/2 + M\left(l + dl/2\right)\right)\omega^2}{\sqrt{\left[kl_m^2 - J\omega^2\right]^2 + \left[\left(c_m + c_{R_i} + c_{R_l}\right)\omega + 4\tau_s/\pi\Theta\right]^2}} \tag{3}$$

The term $4\tau_s/\pi\Theta$ represent the describing function of the coulomb friction. The coefficients c_{Ri} is the contribution of the electrical resistance to the viscous damping and it is

$$c_{Ri} = \frac{K_t^2 R_i}{\left(R_i + R_l\right)^2} \tag{4}$$

while c_{Rl} is the electrical viscous damping produced by the load resistance

$$c_{Rl} = \frac{K_t^2 R_l}{\left(R_i + R_l\right)^2} \tag{5}$$

However, even though they both generate damping, c_{Rl} is responsible for the harvested power produced by the voltage across the load resistance, while c_{Ri} contributes to the dissipations. For the energy harvesting, it is well-known [12] that the power can be increased by selecting a larger mass, because, at resonance, the output increases as confirmed in equation (3). However, in practical applications, due to the limitations on the throw, the mass cannot be as big as one wants. Therefore, the design is usually carried out in the worse conditions scenario, where the system, excited at resonance f_{res} at the maximum input amplitude Y_{max}, responses with the maximum throw Θ_{max}.

2.1. Constrainted design

As aforementioned, the throw is the main, but not the only, constraint that has to be respected. The design of an energy harvester should take into account the environment and the type of excitation. In this case, the environment represents the shaker, and the excitation is harmonic. According to the characteristic of the shaker, it is chosen to have a harvester that resonates at 10 Hz. This value represents a compromise between the performance of the shaker, which cannot provide the desired base displacement Y_{max} below 7 Hz, and the integrity of the device, which is stressed at too high frequency due to the presence of other modes.
The imposed constraints are the following:

- f_{res}=10Hz;
- Θ_{max}=5.5deg;
- ζ=0.07<√2/2;
- l_m=l/2;
- dl=l/6;
- a/b=2.5;

The first constraint points out that the resonance should not be high so that the gearbox, motor or the other components of the assembly do not interact with the dynamics of the harvester. At the same time, the design is constrained by the shaker, since it does not perform well at low frequencies. The constraint imposed on the swing angle is to make sure that the spring behaves linearly. If the swing angle is large, the spring is subjected to an angular displacement and can behave in a nonlinear manner. The importance of the damping ratio is highlighted in the third constraint. It is known [12] that the mechanical damping should be as small as possible to maximize the harvested power, because the power depends on the square of the swing displacement. Therefore, the system is forced to be underdamped. The value of 0.07 is chosen arbitrarily below √2/2, which is the value over which the second-order system does not resonate. The fourth constraint is the position of the spring l_m, which is

placed along the axial length of the beam, in particular at half of the beam length. If $l_m=l$, the stiffness is very low and then spring can show nonlinear behaviour. On the other hand, if $l_m<<l/2$, the stiffness becomes very high to maintain the resonance at 10Hz, and this may affect the integrity of the structure, since energy would be transmitted to the connection between the beam and the gearbox. The dimension *dl* of the lumped mass should not be too large to avoid flexural modes at low frequency, but, at the same time, it can increase the swing angle, and, therefore, the output voltage. The last constraint ensures similar modes (vertical and horizontal bending modes) are not close to each other in frequency.

The first algebraic equation is referred to the resonance frequency f_{res} as

$$f_{res} = \frac{1}{2\pi}\sqrt{\frac{k l_m^2}{\left(\frac{1}{3}ml^2 + M\left(l+\frac{dl}{2}\right)^2\right)}} \tag{6}$$

The maximum throw Θ_{max} takes place at the natural frequency, when the maximum input is $Y_{max.}$ considered Therefore,

$$\left|\Theta_{\max}\right| = \frac{\left(ml/2 + ML\right)\omega_n^2 Y_{\max}}{\left[\left(c_m + c_{R_i} + c_{R_l}\right)\omega_n + 4\tau_s/\pi\Theta_{\max}\right]} \tag{7}$$

For the damping ratio is then imposed

$$\zeta = \frac{c_m + c_{R_i} + c_{R_l}}{2J\omega_n} \tag{8}$$

The position l_m of the spring is

$$l_m = \frac{l}{2} \tag{9}$$

The edge *dl* of the added mass and the ratio between the cross section dimensions *a* and *b* is

$$dl = \frac{l}{6},\ \frac{a}{b} = 2.5 \tag{10}$$

There are 8 parameters to compute, which are *m*, *M*, *k*, *l*, l_m, *dl*, *a*, *b*. However, the number of equations is six. Therefore, two equations are added, relating the mass of the beam and the lumped mass with their volumes. For the beam, it is

$$m = \rho abl \tag{11}$$

and for the lumped mass is

$$M = \rho(dl)^3 \tag{12}$$

The input parameters, which include also the characteristics of the DC motor (Maxon motor 70W), are presented in Table 1:

Table 1. Input design parameters

Parameter	Value
Coupling coefficient (K_t)	0.0255 Nm/A
Internal resistance (R_i)	0.628 Ω
Load resistance (R_l)	0.628 Ω
mechanical damping (c_m)	0.12 Nsm
Static friction (τ_s)	0.068 Nm
Gear ratio (G)	18
Input displacement (Y)	0.0025 m
Density (ρ)	7700 kg/m^3

In Table 1, the mechanical viscous damping c_m is known and previously estimated by attaching a pendulum to the gearbox and measuring the time decay. The logarithmic decrement method is then applied to the first periods of oscillation (avoiding the friction) and the damping is computed. The value of the estimated damping includes the damping of the gearbox, the motor and pendulum, which is not part of the device. However, this approximate value is used for simulations.
The value of the static friction is estimated separately with a static test. An L-shaped inner hexagonal spanner is fixed to the gear box, and weights are added to the edge until the weight of the mass is higher than the static friction.
It is well-known that there exists an optimum load resistance such that the harvested power is maximized. For constrained energy harvester, it was demonstrated that the optimum condition is achieved when the load equals the internal resistance [7, 12]. Therefore, the harvester is designed according to this result, therefore it is imposed $R_l=R_i$, as shown in Table 1. By solving the previous algebraic system, all the design parameters were computed and a *CAD* model can be built in Solidwork (Figure 2(a)). However, during the manufacturing process some of the parameters were varied and the design parameters were updated according to these modifications.
The updated set of parameters is the reported in Table 2.

Table 2. Design parameters

Parameter	Value
Beam mass (m)	0.45 kg
Lumped mass (M)	0.21 kg
Beam length (l)	0.182 m
Lumped mass length (dl)	0.03 m
Spring position (l_m)	0.092 m
Stiffness (k)	6700 N/m
Cross section, (a)	0.028 m
Cross section, (b)	0.011 m

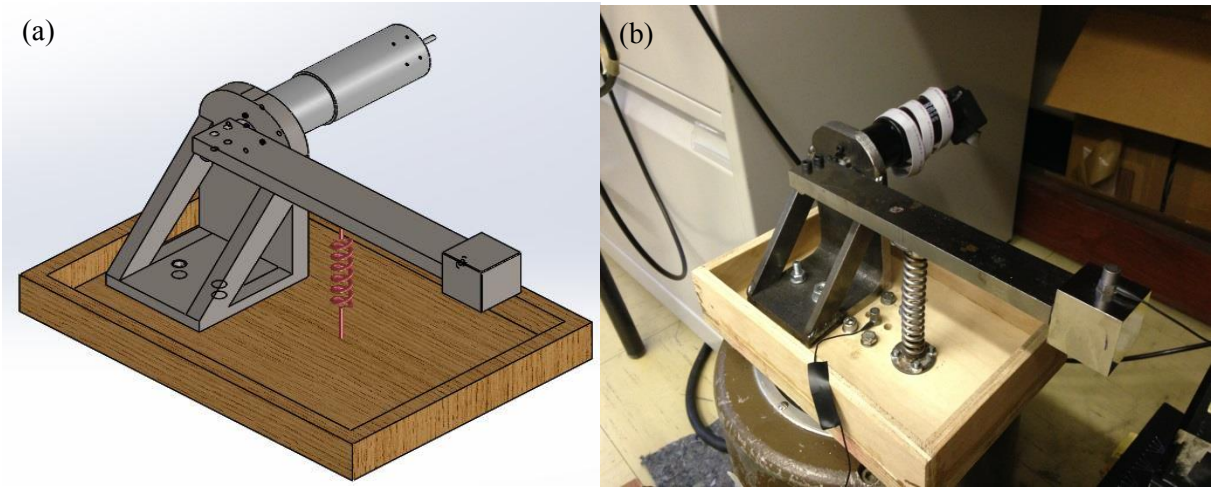

Figure 2: Cad model (a) and test rig (b) of the energy harvester

3. Experimental characteristics of the energy harvester

In this section, the first tests conducted on the energy harvester are shown. They are aimed to evaluate the resonance of the system and the presence of nonlinearity. To do that, a random white noise input signal was sent to the amplifier by the signal generator. The power amplifier supplies power to the shaker, which excites the harvester from the base. Two accelerometers were fixed on the structure, as shown in Figure 2(b). One is placed on the lumped mass, which provides the acceleration of *x*, and one on the base, which reads the acceleration of *y*. The equipment used is listed in Table 3:

Table 3: Equipment for the conducted tests

Equipment	Type
Amplifier	DataPhysics 30W
Shaker	Derrintron Vibrators VP4
Accelerometer	B&K charge type 4375
Acquisition system	LMS Scadas 8 channels

3.1. Detection of nonlinearity

The first set of test is carried out to characterise the dynamics of the harvester. At this stage no electrical load is attached, and the device is in open circuit condition ($R_l \to \infty$). In particular, a random excitation was imposed by the signal generator in the range 5-100Hz and 25 averages were taken. The number of spectral was set at 2048, which implies a frequency resolution of 0.0488Hz and an acquisition time of 20.48 s. This acquisition parameters will be used also for the random test discussed in the next subsection. The test was conducted at different input voltage levels to verify whether nonlinearity was present. The absolute trasmissibility, in Figure 3(a), and the coeherence function, in Figure 3(b), are used to check the precence of the nonlinearity at different input voltages. The absolute transmissibility T_a is obtained experimentally as the ratio between the accelerations measured from the accelerometer x and the accelerometer y.

$$T_a = \frac{\ddot{x}}{\ddot{y}} \tag{13}$$

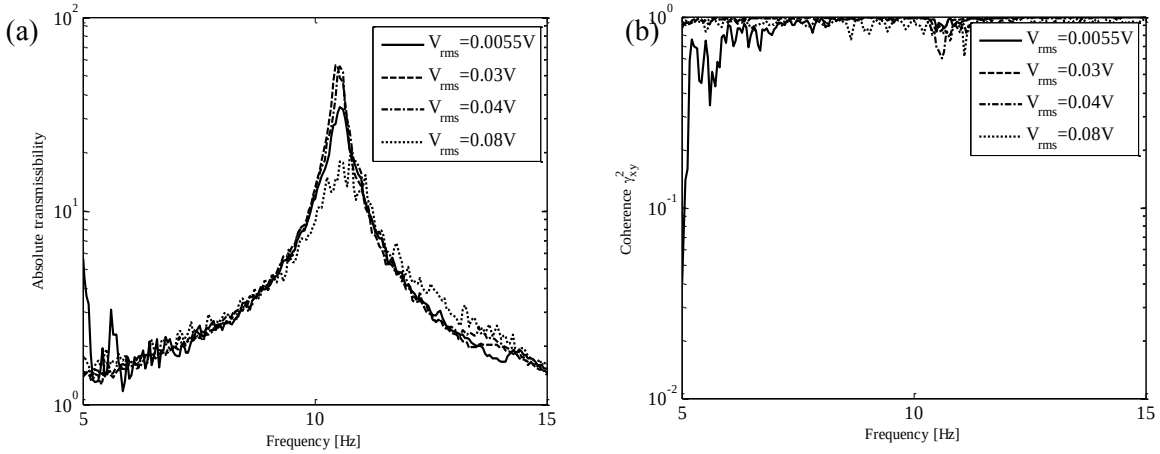

Figure 3: Absolute transmissibility (a) and coherence function (b) for different input levels in the range 5-15 Hz

From the absolute transmissibility in Figure 3(a), it can be seen that the resonance is around 10,3Hz. This value is in agreement with the design estimation and the small variation (0.3Hz) may be due to the variation of some design parameters during the manufacturing process. At a first glance, the system is nonlinear at low inputs due to friction. The absolute transmissibility moves upwards when the voltage is increased from 0.0055V rms (solid black line) to 0.03V rms (dash black line), and it remains constant up to 0.04, which means that the system is linear in this range. At 0.08V, the transmissibility starts dropping again due to a rattling effect, which generates vibration inside the gearbox. In this condition, a bigger increase of input voltage does not produce a larger rotation of the motor shaft, but only larger impacts between the gears. A confirmation of the presence of the rattling effect is given also by the coherence function. Indeed, by looking at the black dotted line in Figure *3*(b), is evident how the coherence drops as a certain amount of the energy introduced into the system is wasted by the impacts between the teeth of the gearbox.

3.2. Influence of the electrical circuit

The previous analyses were made in open circuit condition, which means that, even though a voltage can be detected from the motor, there is no current and therefore the power is zero. On the opposite, in short circuit, the load resistance equals zero, and the current is present, but the voltage equals zero, therefore harvested power is still zero. These two conditions are here analysed together with a load condition (R_l=1Ω) by measuring the time response acceleration *x* of the beam.
Assuming, that the electrical circuit is linear, it expected to see that in open circuit the response is larger since the electrical damping goes to zero in fact

$$c = c_m + \frac{K_t^2}{R_l + R_i} \rightarrow c_m \tag{14}$$

On the other hand, when the circuit is shorted, the load resistance is zero, and

$$c = c_m + \frac{K_t^2}{R_l + R_i} = c_m + \frac{K_t^2}{R_i} \tag{15}$$

As shown by the equation (13) and equation (14), the electrical damping is inversely proportional to R_l and therefore, by increasing the load the damping tends to reduce. The effect of the load on the acceleration *x* is shown in Figure 4.

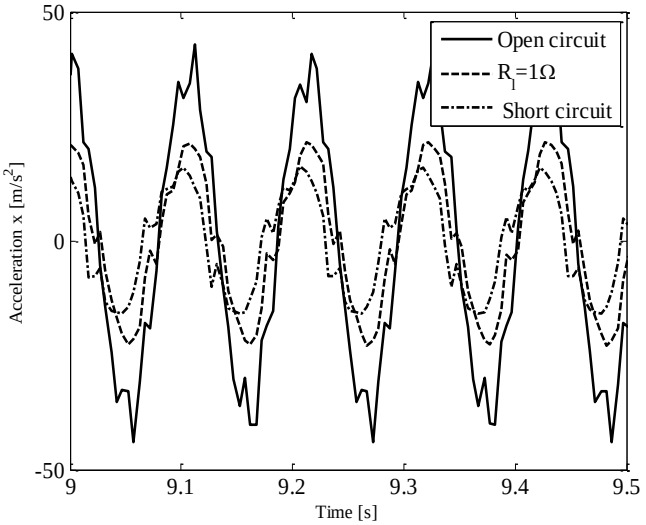

Figure 4: Effect of the load resistance the x-acceleration for a base acceleration – Input V_{rms} = 1.19V

From Figure 4, it can be noticed how the load resistor affects the beam acceleration. To obtain this result, a harmonic test was performed at resonance, in open circuit (black solid line), load circuit (black dash line) and short circuit (black dot line). It is seen that open and short circuits represent extreme conditions and, when a load is attached, the response is placed in between. It can be summarised that the response is expected to have a monotone trend with respect to the load, as also demonstrated in literature [1, 8, 9].

4. Dynamic range of the harvester

As aforementioned, the advantage of implementing a cubic damping is to increase the dynamic range. In other words, when a harmonically base excited harvester is excited at low input levels, the force (or the voltage) acting on the damper (or the electric load resistance) is lower with respect to a linear damper (or the electric load resistance). Therefore, the response is larger and more harvested power is provided. Indeed, recalling the amplitude of the swing angle in frequency domain, in equation (7), it is

$$|\Theta| = \frac{\left[\left(ml/2 + ML\right)Y\omega_n^2 - 4\tau_s/\pi\right]}{\left[\left(c_m + c_{R_i} + c_{R_l}\right)\omega_n\right]} \tag{16}$$

For underdamped structures, the maximum power is obtained at the natural frequency, and it can be related to the swing amplitude as:

$$P_{harv} = E\left[c_{R_l}\dot{\theta}^2\right] = \frac{1}{2}G^2 c_{R_l}\omega^2|\Theta|^2 \tag{17}$$

The harvested power can be computed as the mean value of the damping force, associated with the load resistance, and the velocity. When the load is defined, the power only depends on the square of the amplitude of the swing angle times the frequency of excitation and, it is maximum at resonance.

4.1. Output voltage and harvested power

The electric load contributes to the harvested power. Therefore, the voltage across the load is related to the harvested power. For a linear load resistance, the voltage depends on the swing velocity and is given as

$$V_{Rl}(t) = GK_t \frac{R_l}{R_l + R_i} \dot{\theta}(t) \tag{18}$$

So, the instantaneous power depends on the square of voltage as

$$P_{harv} = E\left[\frac{V_{Rl}^2(t)}{R_l}\right] \tag{19}$$

In Figure 5(a), the voltage across the load is measured at resonance for different load resistances, such as 0.3Ω, 1Ω, 10Ω and 100Ω.

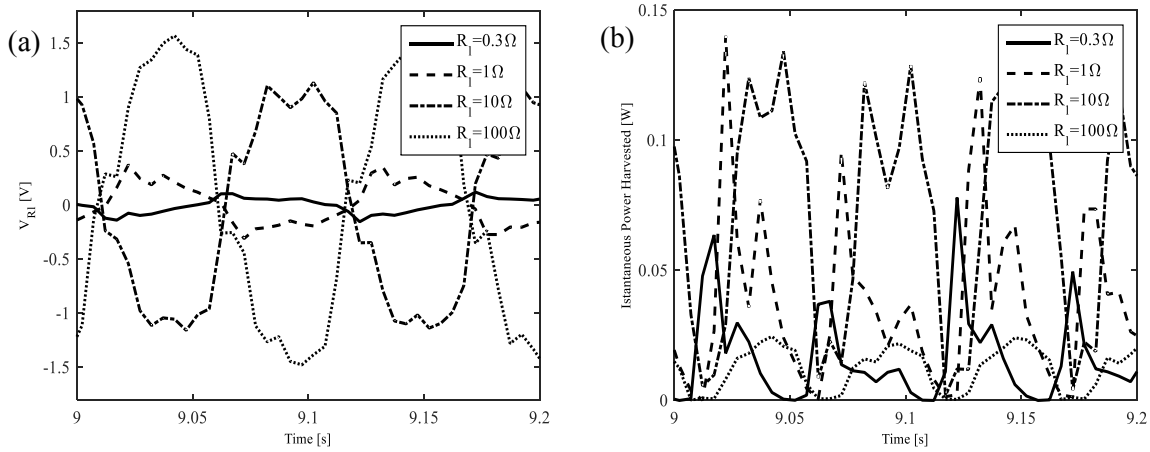

Figure 5: Output voltage (a) and instantaneous power (b) as a function of time for three different load resistors - Input V_{rms} = 1.19V

It can be seen that, by increasing the load, the voltage across R_l tends to go higher. When the load is zero (short circuit), the voltage across the load is zero, even though current passes through the circuit. When the circuit is open, thus $R_l \rightarrow \infty$, an asymptotic condition is achieved, which corresponds to have no current through the circuit, but a non-zero voltage. From Figure 5(b), the instantaneous harvested power is studied as a function of the load. It can be seen that from 0.3Ω to 10Ω, the power increases sharply, and then it drops at 100Ω. As demonstrated [1, 7-9, 11, 12], the harvested power usually shows a peak of power in correspondence of an optimum value of load R_l. The reason is that the electrical damping, shown in equation (5), presents a peak value as a function of the load R_l, as shown in Figure 6. However, since K_t is small, there is not a huge variation of c_{Rl} and, therefore, the peak of power is hard to be detected experimentally.

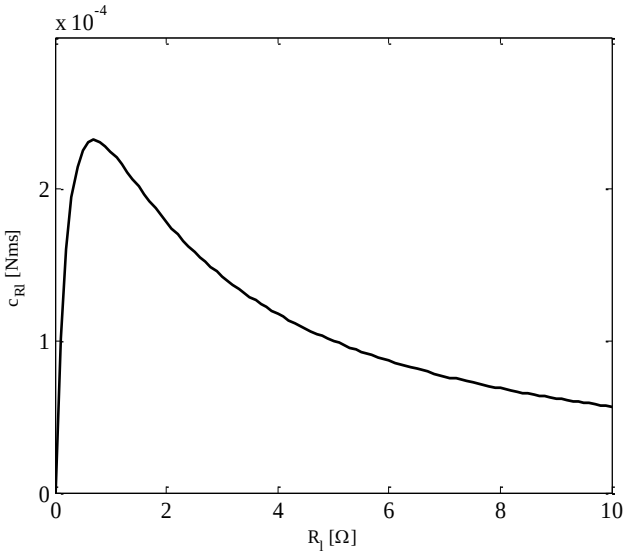

Figure 6: Effect of the load resistance on the viscous damping

4.2. Level curves

The response of the device should be linear in terms of both swing angle and voltage, when the load R_l is imposed, and the device is harmonically excited at different input levels.

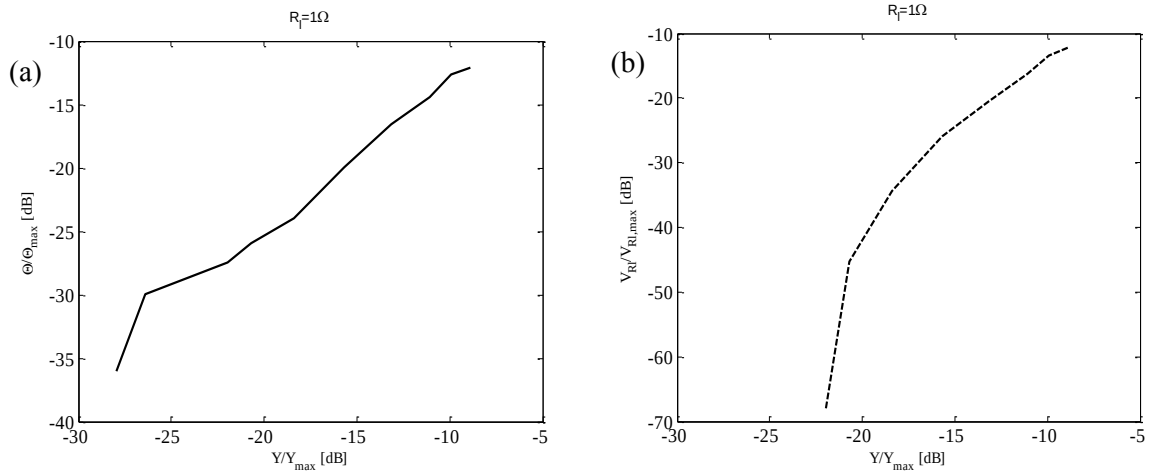

Figure 7: Level curves of swing angle and voltage across the load for different input levels - Θ_{max}=5.5deg and V_{max}=1V

From Figure 7, the system responds linearly both in swing angle and voltage from -20dB onwards. Below -20dB, instead, the system shows nonlinear behaviour, which is associated to the friction. In particular, it can be noticed that the harvester does not provide voltage below -22dB, because the excitation is small and the amount of displacement produced is wasted by friction.
Recalling equation (18), the level curves for the harvested power are provided in Figure 8.

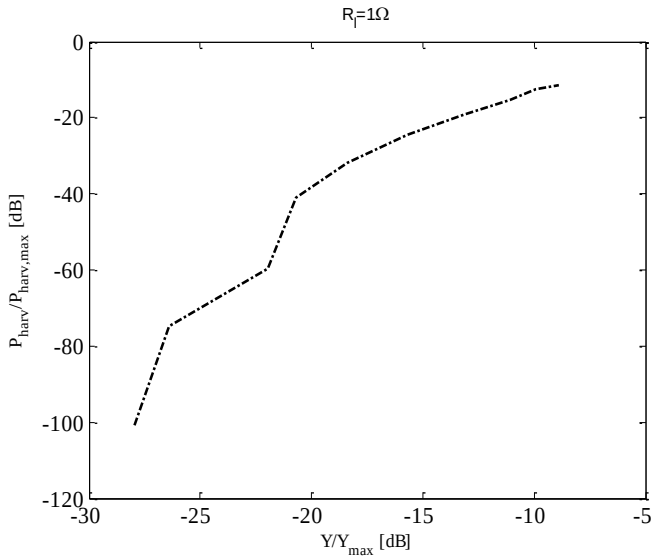

Figure 8: Level curves of the harvested power for different input levels - P_{max}=1W

The presence of the friction, detected in the swing angle and in the voltage, has a strong consequence on the harvested power. The behaviour is similar to what shown in Figure 7. The power is subjected to a huge reduction as the input level is decreased. As a consequence, the level of the input should be kept as large as possible so that a large swing angle would not be affected by friction. Obviously the input level depends on how high the saturation limit of the amplifier is, and how large is the displacement the shaker can provide.

4.3. Future work: mathematical model of a nonlinear energy harvester

The goal of implementing a nonlinear load is to increase the dynamic range of the harvester. By deliberately introducing nonlinearity into the electrical circuit, it is expected a variation of the performance, especially at low input levels. The algebraic equation describing the dynamics of the electrical circuit assumes now the following form

$$K_t \dot{\theta} = (R_l i)^{1/3} + R_i i \tag{20}$$

This equation is a third-degree algebraic polynomial in i with three solutions, in which only one is real, and is

$$\mathrm{i(t)} = \frac{1}{6}\left[\frac{6K_t\dot{z}}{R_l} + \left(-54K_tR_i^5R_l\dot{z} + 6\sqrt{3}\sqrt{R_i^9R_l^2\left(4R_l + 27K_t^2R_l\dot{z}^2\right)}\right)^{1/3} \left(\frac{2^{1/3}}{R_i^3} - \frac{3^{1/3}2R_l}{\left(-9K_tR_i^5R_l\dot{z} + \sqrt{3}\sqrt{R_i^9R_l^2\left(4R_l + 27K_t^2R_l\dot{z}^2\right)}\right)^{2/3}}\right)\right] \tag{21}$$

Analyses are being currently run on this model and will be presented in future publications.

5. Conclusions and future work

The present paper shows the design and the tests of an electromagnetic transducer energy harvester, which is aimed to transform the energy provided by the base motion into harvested power. The design process was conducted by imposing constraints aimed to guarantee the correct operative conditions. First tests were conducted to analyse the dynamics of the system in open circuit. Random white noise input was used to excite the system at different input levels. Results show nonlinear behaviour at low input levels, which is associated with the friction inside the gearbox and at high input levels, related to rattling phenomena. The effect of the load is then considered. The device was

subjected to a harmonic base excitation at resonance, and the response of the system, in terms of swing acceleration x and voltage was studied at different loads. The introduction of an electrical resistance R_l acts on the viscous damping of system, and it results in an intermediate condition between open circuit ($R_l \rightarrow \infty$) and short circuit ($R_l=0$). For harmonic excitation with a constant input level of excitation, the voltage across the load and the swing angle tend to get larger as long as the resistance increases, because the viscous damping is inversely proporsional to R_l. The detection of the nonlinearity was also investigated with variable input levels. Assuming a constant load R_l, the system was harmonically tested at different inputs Y_{max}. It was shown that the presence of friction mainly affects the system at low input levels and the system behaves linearly as long as the input increases. The nonlinearity was evident in the swing angle as well as the voltage and the harvested power. In particular, the harvested power drops dramatically for low input level, therefore the input should be kept as high as possible (according to the performance of the shaker and of the amplifier) to produce a higher swing angle and to increase the effect of the coupling on the harvested power. Future works will be focused on improving the design to obtain a better coupling between the electrical and the mechanical circuits and on the updating of the mathematical model, especially of the damping force, and on a comparison with the experimental results. Also, the experimental implementation of a cubic load represents a crucial step to demonstrate the effectiveness of the approach proposed in the last subsection.

6. Aknowledgment

The work here presented was funded by the EPSRC through the 'Engineering Nonlinearity' program (EP/K003836/1).

7. References

[1] M Hendijanizadeh, Design and optimisation of constrained electromagnetic energy harvesting devices, PhD dissertation, University of Southampton, 2014;
[2] T J Sutton, S J Elliott, M J Brennan, K H Heron, D A Jessop, Active isolation of multiple structural waves on a helicopter gearbox support strut, Journal of Sound and Vibration, vol. 205, 81–101, 1997;
[3] C B Williams, R B Yates, Analysis of a micro-electric generator for microsystems, Sensors and Actuators, 8 – 11, 1996;
[4] B P Mann, N D Sims, Energy harvesting from the nonlinear oscillations of magnetic levitation, Journal of Sound and Vibration, vol. 319, 515-530, 2009;
[5] M Ghandchi Tehrani, S J Elliott, Extending the dynamic range of an energy harvester using nonlinear damping, Journal of Sound and Vibration, vol. 333, 623–629, 2014;
[6] L Simeone, M G Tehrani, S J Elliott, M. Hendijanizadeh, Nonlinear damping in an energy harvesting device, ISMA 26th International Conference, 2014;
[7] N G Stephen, On energy harvesting from ambient vibration, Journal of Sound and Vibration, 409 – 425, 2006;
[8] M Hendijanizadeh, S M Sharkh, S J Elliott, M Moshrefi-Torbati, Output power and efficiency of electromagnetic energy harvesting systems with constrained range of motion, Journal of Smart Materials and Structures, vol. 22, 125009 (10pp), 2013;
[9] M Hendijanizadeh, M Moshrefi-Torbati, S M Sharkh, Constrained Design Optimization of Vibration Energy Harvesting Devices, Journal of Vibration and Acoustics, vol. 136, 1 – 6, 2014;
[10] O L Green, K Worden, K Atallah, N D Sims, The benefits of Duffing-type nonlinearities and electrical optimisation of a mono-stable energy harvester under white Gaussian excitations, Journal of Sound and Vibration, vol. 331, 4504 – 4517, 2012;
[11] M Hendijanizadeh, S J Elliott, M Ghandchi Tehrani, The effect of the internal resistance on an energy harvester with cubic resistance load, ICSV22 The 22nd International Congress on Sound and Vibration, 12-16 July, 2015;
[12] M Hendijanizadeh, Constrained design optimisation of vibration energy harvesting devices, Journal of Vibration and Acoustics, vol. 136/021001-1-6, 2014;